ACS OMEGA

Open Access

http://pubs.acs.org/journal/acsodf

Article

Deubiquitination Detection of p53 Protein in Living Cells by Fluorescence Cross-Correlation Spectroscopy

Yaoqi Liu, Chaoqing Dong,* and Jicun Ren*

Cite This: *ACS Omega* 2023, 8, 36588−36596

Read Online

ACCESS | Metrics & More | Article Recommendations | Supporting Information

ABSTRACT: Deubiquitination is a reverse post-translational modification of ubiquitination and plays significant roles in various signal transduction cascades and protein stability. The p53 is a very important tumor-suppressor protein and closely implicates more than 50% of human cancers. Although extracellular studies on the deubiquitination of p53 were reported, the process of p53 deubiquitination in living cells due to the shortage of an efficient in situ method for single living cells is still not clear. In this study, we described an in situ method for studying p53 deubiquitination in living cells by combining fluorescence cross-correlation spectroscopy with a fluorescent protein labeling technique. We first constructed the stable cell line expressing EGFP-Ub-p53-mCherry as the substrate of p53 deubiquitination. Then, we established a method for in situ monitoring of the deubiquitination of p53 in living cells. Based on the amplitudes of fluorescence correlation spectroscopy and fluorescence cross-correlation spectroscopy curves from living cells, we obtained the deubiquitination percentage for evaluating the level of p53 protein deubiquitination. Furthermore, we studied the effects of ubiquitin structures on p53 deubiquitination in living cells and found that the C-terminal Gly75-Gly76 motif of ubiquitin is a key location for p53 deubiquitination and the deubiquitination cannot occur when ubiquitin lacks the C-terminal Gly75-Gly76 motif. Our results documented that the developed strategy is an efficient method for in situ study of deubiquitination of proteins in living cells.

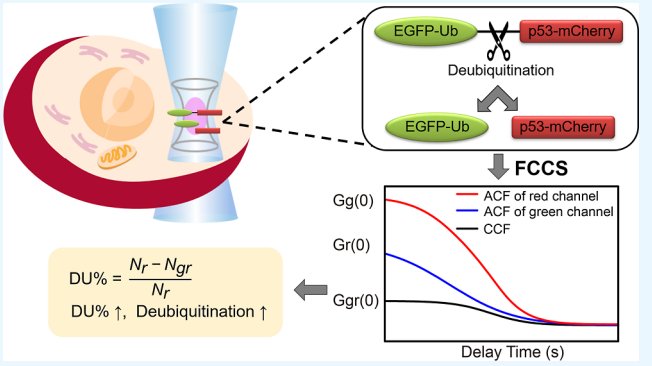

INTRODUCTION

Ubiquitin (Ub) is a highly conserved, 76 amino acid polypeptide ubiquitously expressed in eukaryotic cells.[1] Ubiquitination is a reversible post-translational modification involved in the regulation of most cellular processes. Conjugation of the ubiquitin C-terminal Gly−Gly motif to lysine residues or the N-terminal on target proteins relies on the sequential activity of Ub-conjugating enzymes (E1, E2, and E3).[2] On the contrary, Ub was removed from target proteins by the recognition of deubiquitinases (DUBs, also known as deubiquitylating or deubiquitinating enzymes). Deubiquitination is as important as ubiquitination in cell life activity.[3] The balance of ubiquitination and deubiquitination regulates several key cellular processes, including protein degradation,[4] vesicular trafficking,[5] DNA repair,[6,7] endocytosis,[8] and various signaling pathways.[9] Therefore, the study of deubiquitination is very important to understand some physiological and pathological processes.

The p53 protein is a tumor suppressor protein and plays essential roles in cell cycle arrest, DNA repair, angiogenesis, autophagy, migration, aging, senescence, and apoptosis.[10−12] The p53 protein is a central governor of various critical cellular processes which is modulated by a large number of post-translational modifications,[13,14] such as ubiquitination and deubiquitination.[15] DUBs can regulate the p53 signaling pathway in response to different stresses.[16−18] In previous studies, various traditional methods have been used to research the deubiquitination of p53. Western blotting and coimmunoprecipitation are the most frequently used methods for studying the deubiquitination of p53, and they can conveniently catch the tendency of ubiquitinated p53 protein from the brightness of protein bands.[19,20] The polymerase chain reaction is also a good way to monitor the expression of p53.[21] Mass spectrum is a powerful method for the detection of semisynthetic products, such as ubiquitinated proteins[22] or site-specific chemical probe.[23] Flow cytometry is also used to recognize the cells in different cell cycles or different cellular states.[24] Although certain progress was made, few researches give the direct information on deubiquitination of p53 in single living cells under physiological conditions due to lack of an efficient and in situ method. Currently, there still remain many challenges in in situ monitoring of deubiquitination of p53 in

Received: August 18, 2023
Accepted: September 7, 2023
Published: September 22, 2023

living cells due to the quite complex environment of living cells.

In recent years, single-molecule technologies have provided an unprecedented way to study the behavior of biological molecules. Single-molecule force measurements,[25,26] single-molecule Fürster resonance energy transfer,[27,28] single-molecule counting,[29] and fluorescence correlation spectroscopy[30] are the most commonly used methods. Fluorescence correlation spectroscopy (FCS) and fluorescence cross-correlation spectroscopy (FCCS) are highly sensitive single molecule detection techniques which are widely used in the in situ study of certain biological processes in living cells. Currently, we applied FCS/FCCS to study molecular interactions in solution and in a single living cells including the protein−protein interactions, RNA−protein interactions, and drug−protein interactions.[31] Peng et al. revealed target search and recognition mechanisms of glycosylase AlkD by combining scanning FRET-FCS with the Markov state model.[32] Sandberg et al. identified a photoisomerized, red-shifted emissive state in SCy7 (Sulfo-Cyanine7) by a combination of FCS and transient state (TRAST) excitation modulation spectroscopy.[33] Sankaran et al. implement a GPU-supported, camera-based measurement strategy to achieve simultaneous spatiotemporal super-resolution and multiparametric fluorescence microscopy from a single fluorescence data set.[34] However, to our knowledge, we have not found any reports about in situ study of protein deubiquitination in living cells.

In this work, we report a new method for in situ study of deubiquitination of p53 protein in living cells by combining FCCS with a fluorescent protein labeling technique. We first constructed the substrates of p53 deubiquitination containing Ub fused with EGFP and mCherry (EGFP-Ub-p53-mCherry). EGFP-Ub-p53-mCherry were stably expressed in H1299 by using a lentiviral transfection technique. This p53 protein can be deubiquitinated by endogenous DUBs of living cells, and FCCS was used to measure the level of p53 deubiquitination. The deubiquitination percentage (DU %) was calculated for evaluating the level of deubiquitination according to the amplitudes of FCS and FCCS curves from living cells, and it is positively correlated to the level of deubiquitination. Furthermore, we studied the effects of Ub structures on p53 deubiquitination and found that the C-terminal Gly75-Gly76 motif and Ile44 hydrophobic patch are essential for deubiquitination of p53 in living cells. This strategy provided an efficient method for in situ study of protein deubiquitination in a single living cell.

EXPERIMENTAL SECTION

Materials and Instruments. Human embryonic kidney (HEK293T) cell line and human non-small cell lung cancer cell line (H1299) were obtained from American Type Culture Collection (USA). 1× Glo Lysis buffer was supplied by Promega Biotech Co., Ltd. (China). RPMI 1640 medium, Dulbecco's modified Eagle's medium (DMEM), and fetal bovine serum (FBS) were products of Corning Incorporated (USA). Penicillin/streptomycin, trypsin, glucose, sodium pyruvate, minimal essential medium (Opti-MEM), and lipofectamine 3000 were supplied by Thermo Fisher Scientific (USA). Cover glass bottom imaging dishes were purchased from MatTek (USA). Phosphate-buffered saline (PBS) powder was from Sangon Biotech (Shanghai) Co., Ltd. (China). Anti-His antibody (abs830002), anti-β-actin antibody (abs100041), antimouse antibody (abs20001), antirabbit antibody (abs20040), anti-GFP antibody (abs124040), and anti-mCherry antibody (abs149627) were purchased from Absin Bioscience Inc. (China). Genomic DNA extraction kits were purchased from Thermo Fisher Scientific (USA) (K182001).

Construction of Plasmids and Mutants. A series of plasmids and mutants of Ub and p53 were constructed. Plasmid pLVX-EGFP-Ub-p53-mCherry was constructed with enhanced green fluorescent protein (EGFP), Ub, p53, and mCherry, which were fused and cloned into lentiviral vector pLVX, and His-tag was added to its C-terminus and N-terminus, respectively. Plasmid pLVX-EGFP-p53-mCherry was constructed as a control group which lacks the Ub gene in comparison to pLVX-EGFP-Ub-p53-mCherry. We also constructed pLVX-EGFP[35] and pLVX-mCherry as the blank group. To fully understand the deubiquitination of p53, we constructed two Ub mutant plasmids. pLVX-EGFP-Ub-p53-mCherry-ΔGG lacked two C-terminal glycines of Ub, and pLVX-EGFP-Ub-p53-mCherry-MUT mutated the Ile44 hydrophobic patch of Ub (L8A, I44A, H68A, V70A). The details of plasmids construction are described in the Supporting Information.

Cell Culture and Transfection. HEK293T cells were cultured in DMEM with 10% fetal bovine serum and 1% penicillin/streptomycin in a 37 °C humidified incubator with 5% CO_2. H1299 cells were cultured in RPMI 1640 with 10% fetal bovine serum, 1% penicillin/streptomycin, 1.5 g/L $NaHCO_3$, 2.5 g/L glucose, and 0.11 g/L sodium pyruvate in a 37 °C humidified incubator with 5% CO_2. All the plasmids and mutants were stably expressed in H1299 cells by lentiviral transfection. Lipofectamine 3000 and second-generation lentiviral packaging plasmids psPAX2 and pMD2.G were used to obtain the lentiviruses. At first, 125 μL of Opti-MEM and 3.75 μL of lipofectamine 3000 were mixed in tube 1. Target plasmids (1 μg) and lentiviral plasmids (2.25 μg of psPAX2 and 0.75 μg of pMD2.G) were added to 125 μL of Opti-MEM in tube 2 and then p3000 (8 μL) was mixed to tube 2. Next, the solution in tube 1 was gently mixed with tube 2 and incubated for 5 min at room temperature. Then, the mixture was added to HEK293T cells. The lentivirus produced by HEK293T was collected every 24 h and collected two times. The lentivirus was filtered by a 0.45 μm filter member, and 500 μL of lentivirus was added into H1299 cells. After incubation for 72 h, the cells were selected by adding 2 μg/mL puromycin. After 5 days, the H1299 cells stably expressing target proteins were finally obtained.

Laser Confocal Fluorescent Imaging and FCCS Measurement. Cell imaging or FCCS measurement were performed on a homemade FCCS instrument, which was based on the confocal optical configuration.[17] Prior to measurements, living cells were grown in a culture dish with cover glass as the bottom 12 h in advance. During confocal fluorescent imaging or FCCS measurements, the culture dish was moved into a microscope stage incubator placed above the objective lens and living cells were maintained in 5% CO_2 at 37 °C. The confocal imaging was completed by controlling the 3D nanopositioning system (E-712.3CD, Physik Instrumente, Germany) and the detection system of FCCS instrument. Images were obtained and Pearson's colocalization coefficient (PCC) was derived from coloc2 plug-in of ImageJ software (Fiji) to assess the degree of colocalization between EGFP and mCherry.[36] The average PCC was calculated of the cell nucleus from 10 cells. Then, the FCCS measurements were

https://doi.org/10.1021/acsomega.3c06078
ACS Omega 2023, 8, 36588−36596

Scheme 1. Principle for Detection of p53 Protein Deubiquitination in Living Cells by Using FCCS

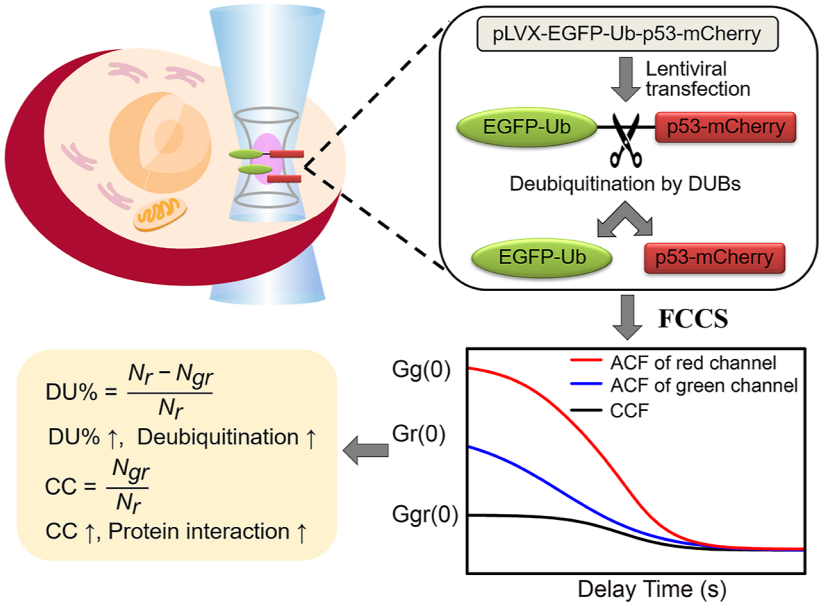

conducted after the objective lens was moved to the target position by controlling the nanopositioning system based on the obtained confocal fluorescent image of cells. The acquisition time was 10 s and repeated six times. About 10 cells were tested under identical conditions. The autocorrelation curves of the proteins fused with EGFP or with mCherry were obtained in the green or red detection channels (G_g or G_r), respectively. The obtained raw data of autocorrelation curve were nonlinearly fitted with the software (Origin 8.0, OriginLab, USA) using the anomalous diffusion model of FCS in living cells (eq 1).[37,38] The theory of FCS is shown in the Supporting Information.

$$G(\tau) = \frac{1}{N}\left(1 + \frac{T e^{-\tau/\tau_{tr}}}{1-T}\right)\frac{1}{1+\left(\frac{\tau}{\tau_D}\right)^{\alpha}}\frac{1}{\sqrt{1+\left(\frac{\omega_0}{z_0}\right)^2\left(\frac{\tau}{\tau_D}\right)^{\alpha}}} + 1 \quad (1)$$

Where N and τ_D represent the average number and characteristic diffusion time of fluorescent molecules in the focal detection volume. ω_0 and z_0 represent the lateral and axial radii of the focal detection volume. T and τ_{tr} represent the fractions and delay times of the fluorescent molecules in the triplet state. α represents the abnormal behavior of fluorescent molecules.[39,40]

In FCCS measurements, cross-correlation function is described in eq 2.[41,42] The cross-correlation curve was measured based on the cross-correlation analysis on the obtained signal fluctuation in the green or red channels.

$$G_{gr}(\tau) = \frac{N_{gr}}{N_g N_r}\frac{1}{1+\frac{\tau}{\tau_D}}\frac{1}{\sqrt{1+\left(\frac{\omega_0}{z_0}\right)^2\frac{\tau}{\tau_D}}} + 1 \quad (2)$$

Wherein N_r represents the average number of red fluorescent molecules that was fitted from the autocorrelation curve of proteins fused with mCherry in the red channel. N_r also represents the total number of EGFP-Ub-p53-mCherry and free p53-mCherry in deubiquitination. N_g represents the average number of green fluorescent molecules, which was fitted from the autocorrelation curve of proteins fused with EGFP in the green channel. N_g also represents the total number of the EGFP-Ub-p53-mCherry and free EGFP-Ub. N_{gr} represents the average number of proteins confused with EGFP and mCherry (herein, EGFP-Ub-p53-mCherry). τ_D is the characteristic diffusion time of EGFP-Ub-p53-mCherry in the detection volume.

The DU % value is defined to represent the deubiquitination percentage of p53, and it is proportional to the degree of deubiquitination. DU % is calculated by eq 3.

$$\text{DU \%} = \frac{\text{The number of deubiquitinated p53 proteins}}{\text{The number of total p53 proteins}} = \frac{N_r - N_{gr}}{N_r} \quad (3)$$

Cross-correlation value (CC) represents the degree of interaction between proteins in the green and red channels. CC value is calculated by eq 4.[43] In this study, the CC value was also used to represent the level of protein deubiquitination.

$$\text{CC} = \frac{\text{The number of interacting parts}}{\text{The number of total substrates}} = \frac{N_{gr}}{N_r} \quad (4)$$

RESULTS AND DISCUSSION

In Situ Measurement Strategy for the Deubiquitination of p53 Protein in Living Cells. Scheme 1 shows the principle for detection of p53 protein deubiquitination in living cells with the FCCS technique. First, the lentiviral plasmid pLVX-EGFP-Ub-p53-mCherry was constructed as the experimental group. Full-length human Ub was fused to the N-terminus of p53 as monoubiquitinated p53 protein (Ub-p53). Also, EGFP and mCherry as fluorescent probes were fused at the Ub-p53 N-terminus and C-terminus, respectively (EGFP-Ub-p53-mCherry). The plasmid without Ub (pLVX-EGFP-p53-mCherry) was constructed as a control group, and plasmids of pLVX-EGFP and pLVX-mCherry were constructed as the blank group. Second, the stable cell lines were constructed by lentiviral transfecting the plasmids into

https://doi.org/10.1021/acsomega.3c06078
ACS Omega 2023, 8, 36588−36596

H1299 cells. Here, EGFP-Ub-p53-mCherry was stably expressed in H1299 cells as the experimental group. Meanwhile, H1299 cells stably expressing EGFP-p53-mCherry (control group) or expressing EGFP and mCherry (blank group) were also constructed. Third, the confocal scanning fluorescence images of these cells were collected with combination of the photon signal in the FCS detection with 3D positioning information from the 3D nanopositioning system. Then, the autocorrelation curves (ACF, Scheme 1, blue and red curves) in the green and red detection channels and their cross-correlation curves (CCF, Scheme 1, black curve) between two channels were determined at the random location by moving the objective lens to the target position within the single living cell with the nanopositioning system. The positions are selected based on the yellow color in the merge confocal image. The CCF curves were obtained due to the synchronous motion of EGFP-Ub-p53-mCherry. The increase in the two color complexes resulted in the increase in the amplitude of the CCF curve [$G_{gr}(0)$]. Finally, the curves were nonlinearly fitted with eqs 1 and 2. The DU % and CC values were calculated with eqs 3 and 4, based on the obtained N_r, N_g, and N_{gr} values in the fittings.

In the experimental group (EGFP-Ub-p53-mCherry), if deubiquitination of p53 did not happen in living cells, EGFP will be well linked with mCherry, and the signals of EGFP and mCherry will be synchronized. In this case, high $G_{gr}(0)$ of CCF curve resulted in low DU %. On the contrary, when deubiquitination of p53 occurred in living cells, Ub was removed from the N-terminus of p53 by endogenous DUBs, and the signals of free EGFP and mCherry were no longer be synchronized. With the deubiquitination level increased, lower $G_{gr}(0)$ of CCF curve resulted in higher DU %. Therefore, DU % reflected the deubiquitination level of p53, and the increase in DU % meant the increase in the deubiquitination level of p53. However, the CC value was negatively correlated to the deubiquitination level of p53.

Deubiquitination of p53 Protein Characterized by the Confocal Imaging Technique and Western Blotting. Typical confocal microscopy images of H1299 cells stably expressing EGFP-Ub-p53-mCherry are shown in Figure 1A1−3. H1299 cells as a host cell were transfected with the plasmid of pLVX-EGFP-Ub-p53-mCherry. The p53 protein is an important transcriptional factor and mainly locates in the cellular nucleus.[44] As shown in the red channel, the p53 is mainly distributed in the cellular nucleus, which was in accordance with the previously reported.[17] In comparison, Ub is distributed in the whole cell, as shown in the green channel. Fluorescent image colocalization analysis (Figure 1B) shows that the PCC of cell nucleus in EGFP-Ub-p53-mCherry cell line is 0.67 ± 0.14 (white dashed circles in Figure 1A3). It is a reasonably strong correlation, and it seems that EGFP-Ub-p53-mCherry has been expressed in the cellular nucleus.

As a comparison, a control group was also constructed. Here, H1299 cells were transfected with the plasmid of EGFP-p53-mCherry, as shown in Figure 1A4−6. Obviously, both mCherry and EGFP were mainly expressed in the cellular nucleus. The PCC of cell nucleus in EGFP-p53-mCherry cell line is 0.95 ± 0.04 (white dashed circles in Figure 1A6). The strong correlation indicated that EGFP-p53-mCherry has been expressed well in the cellular nucleus. The observed results are consistent with the goal of the designed plasmid. Meanwhile, H1299 cells in a blank group were cotransfected with the plasmid mixture of EGFP and mCherry, as shown in Figure 1A7−9. Here, no binding should exist between mCherry and EGFP, which were both uniformly distributed in whole cells. Western blotting of cells stably expressing EGFP and mCherry individually confirmed their expression (Figure 1D). However, the PCC is 0.84 ± 0.10 of the cell nucleus of the EGFP and mCherry cell line (white dashed circles in Figure 1A9). High correlation of the merged image is not consistent with this expectation. As a result, it is difficult to evaluate the deubiquitination of p53 protein from the colocalization image of EGFP-Ub-p53-mCherry.

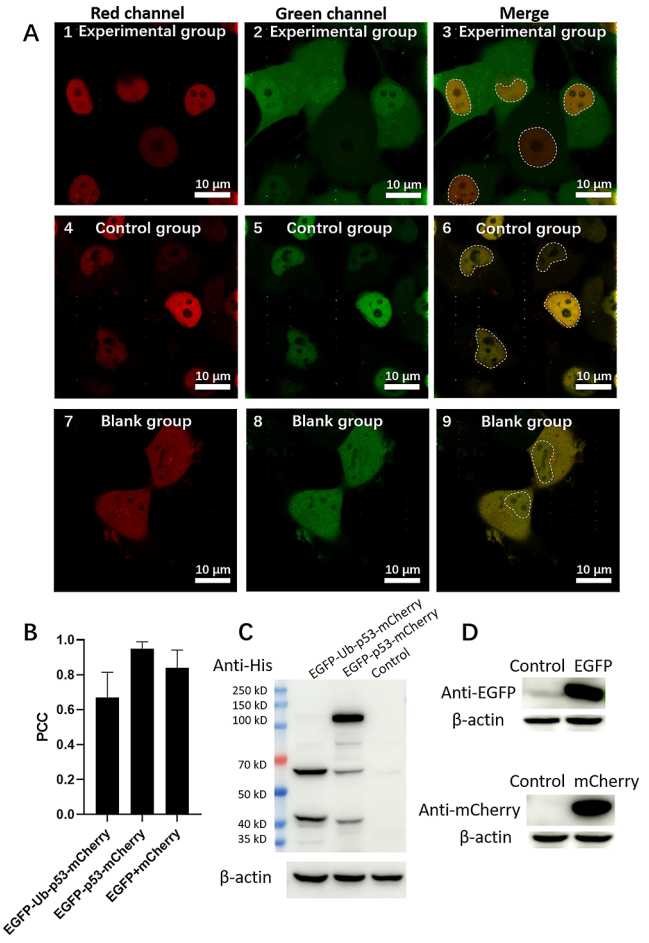

Figure 1. Confocal imaging of stable H1299 cell lines expressing EGFP-Ub-p53-mCherry, EGPF-p53-mCherry, EGFP and mCherry, and protein Western Blotting. (A) Typical confocal microscopy images of cells expressing EGFP-Ub-p53-mCherry (1−3), EGPF-p53-mCherry (4−6), and EGFP and mCherry (7−9), respectively. The scale bars are 10 μm. (B) PCC of cell nucleus of three different cell lines. Data represent means ± the standard deviation. (C) Western blotting of EGFP-Ub-p53-mCherry, EGPF-p53-mCherry, and control (wild-type H1299), and proteins were detected by anti-His antibody. (D) Western blotting of EGFP and mCherry, wild-type H1299 as control, EGFP was detected by anti-EGFP antibody, and mCherry was detected by anti-mCherry antibody.

Western blotting also confirmed this difficulty in the study of the deubiquitination of protein. As shown in Figure 1C, the full-length protein band (≈105 kDa) of EGFP-p53-mCherry was clear in the western blotting image of the control group (second column). However, the weak band of the full length of EGFP-Ub-p53-mCherry (≈114 kDa) was observed in the experimental group (first column in Figure 1C). Also, genomic polymerase chain reaction (Figure S3) analysis can verify the

https://doi.org/10.1021/acsomega.3c06078
ACS Omega 2023, 8, 36588−36596

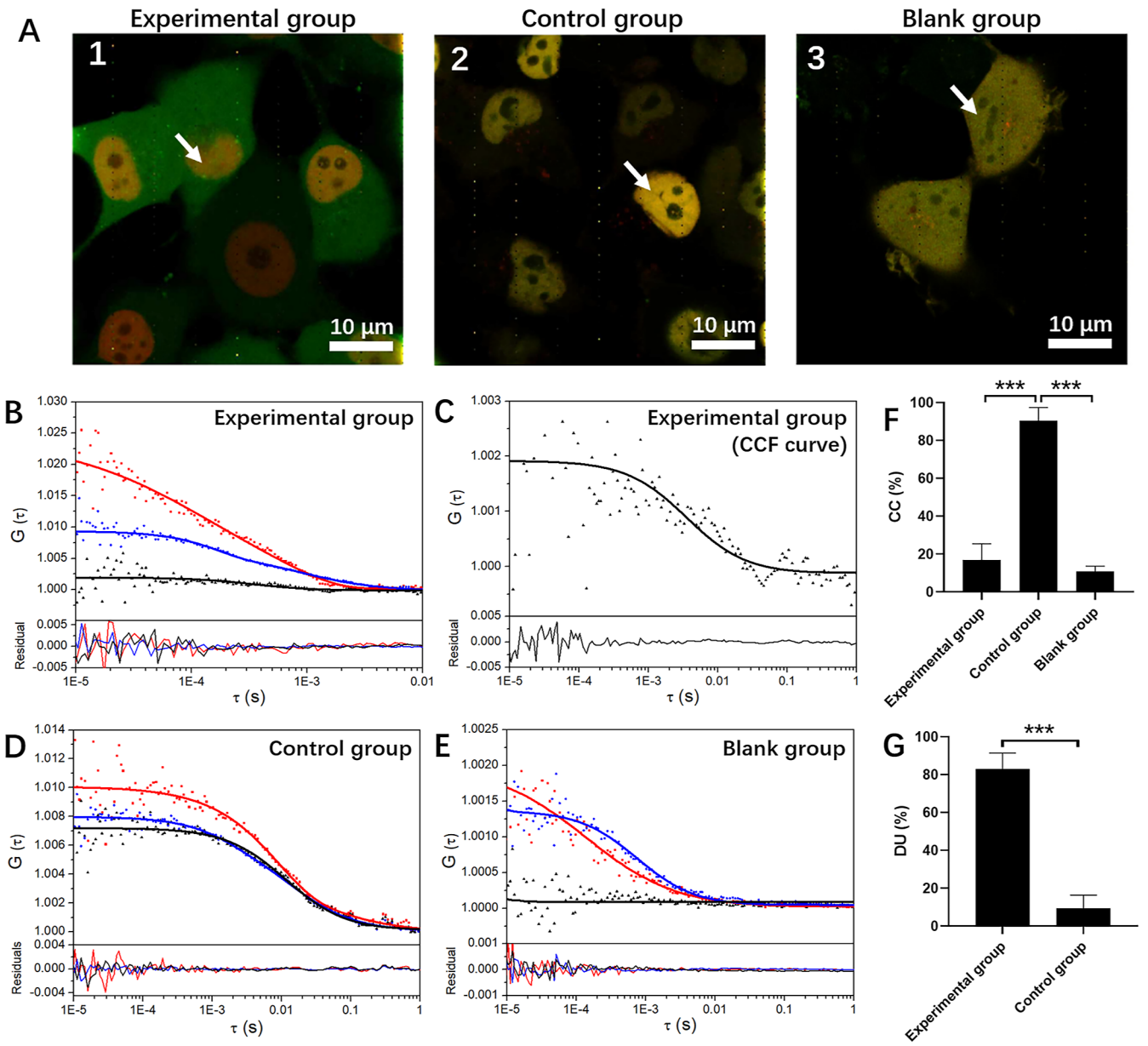

Figure 2. Measurement of the deubiquitination of p53 in living cells by FCS/FCCS. (A) Confocal microscopy images of the experimental group (EGFP-Ub-p53-mCherry), the control group (EGFP-p53-mCherry), and the blank group (EGFP and mCherry), respectively. The white arrows point to the FCCS detection positions of cell nucleus in single living cells. (B) Typical ACF and CCF curves and their fitting residuals of the experimental group in the nucleus of single living cells, respectively. (C) Enlargement of the CCF curve of the experimental group. (D) Typical ACF and CCF curves and their fitting residuals of the control group in the nucleus of single living cells. (E) Typical ACF and CCF curves and their fitting residuals of the blank group in the nucleus of single living cells. (F) Comparison of the CC value of three different cell lines. (G) Comparison of the DU % of the experimental group and the control group. Data represent means ± the standard deviation. Student's *t*-test was used to represent the differences of statistical significance: $*p < 0.05$, $**p < 0.01$, $***p < 0.001$. The results were averaged of 60 measurements from cell nucleus within 10 cells.

successful transfection of EGFP-Ub-p53-mCherry. The above results indicate that cells lines used for deubiquitination research was successfully constructed. However, it is urgent to find a new detection strategy to reveal the deubiquitination process of protein in living cells.

In Situ Measurement of Deubiquitination of p53 in Living Cells by FCCS. With the FCCS measurement strategy, the ACF or CCF curves at the cell nucleus (the yellow position) of the merged image (Figure 2A) within single living cells were measured (Figure 2B–E). Here, the red curve is the ACF curve of the mCherry or proteins labeled with mCherry detected in the red channel. The blue curve is the ACF curve of the EGFP or proteins labeled with EGFP detected in the green channel. Also, the dark curve is the CCF curve of the EGFP and mCherry complex.

Figure 2B,C shows the typical ACF and CCF curves determined at a selected position within the cell nucleus of the experimental group (EGFP-Ub-p53-mCherry). These curves were well fitted with the theoretical models (eqs 1 and 2) and the fitted residuals were below to 0.005. Here, the fitted N_r and N_{gr} values are 48.8 and 10.0 (in Figure 2B,C), respectively. Then, the determined DU % of p53 protein at the position is

https://doi.org/10.1021/acsomega.3c06078
ACS Omega 2023, 8, 36588−36596

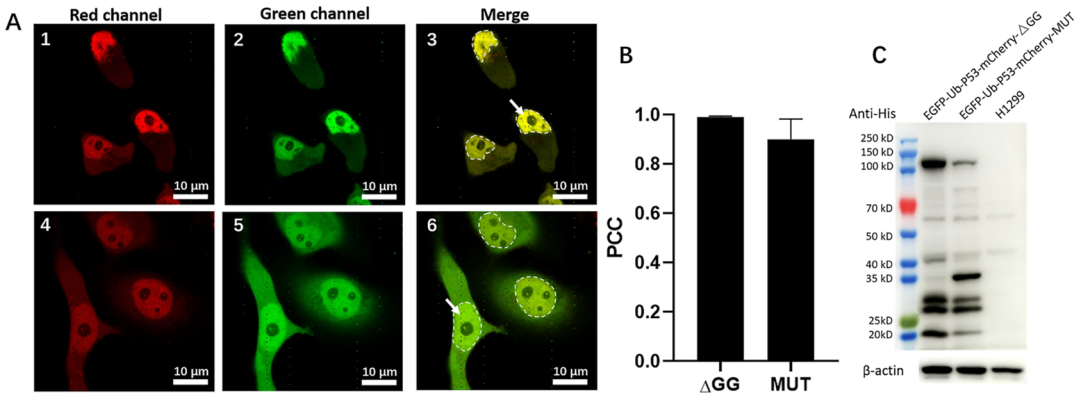

Figure 3. Stable H1299 cell lines expressing EGFP-Ub-p53-mCherry-ΔGG and EGFP-Ub-p53-mCherry-MUT. (A) Typical confocal microscopy images of cells expressing EGFP-Ub-p53-mCherry-ΔGG (1−3) and EGFP-Ub-p53-mCherry-MUT (4−6), respectively. The white arrows point to the FCCS detection positions of the nuclei in single living cells. The scale bars are 10 μm. (B) PCC of cell nucleus of two different cell lines. Data represent means ± the standard deviation. (C) Western blotting of EGFP-Ub-p53-mCherry-ΔGG, EGFP-Ub-p53-mCherry-MUT, and wild-type H1299, and proteins were detected by anti-His.

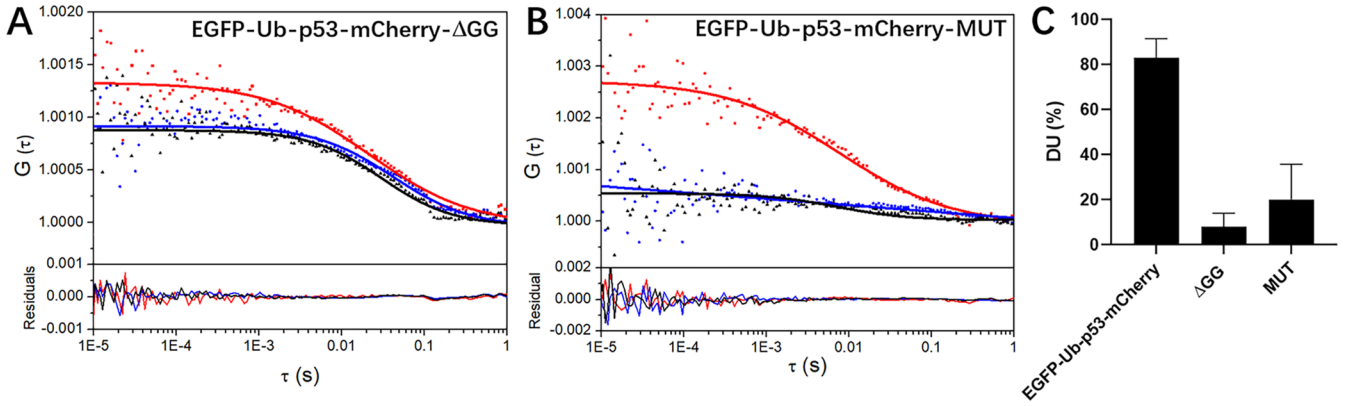

Figure 4. Effects of Ub structures on deubiquitination of p53 in living cells. (A) Typical ACF and CCF curves and curves of fitted residuals of EGFP-Ub-p53-mCherry-ΔGG of a single living cell, respectively. (B) Typical ACF and CCF curves and curves of fitted residuals of EGFP-Ub-p53-mCherry-MUT of a single living cell, respectively. (C) Comparison of the DU % of the experimental group (EGFP-Ub-p53-mCherry) and two different mutants. Data represent means ± the standard deviation. The results were averaged of 60 measurements from cell nucleus within 10 cells.

79.5% based on eq 3. This high DU % value means that the majority of the Ub in the EGFP-Ub-p53-mCherry molecule had been deubiquitinated by endogenous DUBs.

On comparison, using EGFP-p53-mCherry as the control group, its typical ACF and CCF curves in the cell nucleus are shown in Figure 2D. The fitted N_r and N_{gr} values of Figure 2D are 99.7 and 90.2, respectively. The determined CC value is 90.5%. In this case, EGFP-p53-mCherry cannot be cleaved by DUBs as expected because EGFP was not linked with p53 via the Ub molecule.

Meanwhile, when individual EGFP or mCherry were used as a blank group, Figure 2E shows that $G(0)$ of the CCF curve was low due to no linkage between EGFP and mCherry in cells, and the fitted N_r and N_{gr} values were 598.8 and 52.1, respectively. The CC value is only 8.7%, which is mainly from spectral cross-talk in the two channels.

As shown in Figure 2F,G, the average CC and DU % values of different cell lines were compared from a number of cells. The CC value of the experimental group (EGFP-Ub-p53-mCherry), the control group (EGFP-p53-mCherry), and the blank group (EGFP and mCherry) were (17.0 ± 8.5)%, (90.6 ± 6.9)%, and (10.7 ± 2.8)%, respectively (Figure 2F). Low CC value of the experimental group means the signal synchronization of two detection channels is weak. Then, we collected the average DU % of p53 protein in living cells, the DU % of the experimental group and the control group were (83.0 ± 8.5)% and (9.4 ± 6.9)%, respectively (Figure 2G). High DU % of the experimental group indicated that the endogenous DUBs performed well in deubiquitination of p53 proteins in living cells.

The above results suggested that the deubiquitination percentage of the p53 protein in single living cells was measured with the proposed FCCS measurement strategy.

Effects of the Ub C-Terminus and Ub Binding Domain Structure on p53 Deubiquitination. The effects of Ub structures on deubiquitination of p53 in living cells were further studied with the developed measurement strategy. It was reported that the C-terminal Gly75-Gly76 motif[45,46] and Ile44 hydrophobic patch[47−49] of Ub both play a significant role in Ub activity. The Ub C-terminal GG motif is an indispensable part for ubiquitination and deubiquitination, which can be covalently linked to various Ub enzymes and cellular proteins. Except of covalent interactions, noncovalent interactions with Ub mediate a variety of functions[50] and most Ub-binding domains interact with a solvent-exposed hydrophobic patch centered around Ile44 which located in Ub's β-sheet. However, at present, there are few reports about the

https://doi.org/10.1021/acsomega.3c06078
ACS Omega 2023, 8, 36588−36596

effects of Ub structures on deubiquitination using in situ analysis methods.

Here, two mutant plasmids of Ub were constructed. In EGFP-Ub-p53-mCherry-ΔGG, the C-terminal Gly75-Gly76 motif was removed. However, in the EGFP-Ub-p53-mCherry-MUT, the Ile44 hydrophobic patch is mutated (L8A, I44A, H68A, and V70A). These plasmids were transfected into H1299 cells by using lentiviral transfection. Confocal microscopy images (Figure 3A) and Western blotting (Figure 3C) results demonstrated that two plasmids were successfully expressed in H1299 cells. As shown in Figure 3A, in the cells expressing EGFP-Ub-p53-mCherry-ΔGG and EGFP-Ub-p53-mCherry-MUT, fluorescence proteins (EGFP and mCherry) mainly distributed in the cell nucleus and the fluorescence in the cell cytoplasm is low. As shown in Figure 3B, PCC of cell nucleus in EGFP-Ub-p53-mCherry-ΔGG cells and EGFP-Ub-p53-mCherry-MUT cells are (0.99 ± 0.01)% and (0.90 ± 0.08)% (white dashed circles in the merged image of Figure 3A), respectively. Strong correlation of two cell lines indicated that the red channel and the green channel were well colocalized in the confocal image. However, it is also difficult to distinguish the deubiquitination level of p53 in living cells based on the results of confocal microscopy images and western blotting.

Figure 4A,B shows the ACF or CCF curves of EGFP-Ub-p53-mCherry-ΔGG and EGFP-Ub-p53-mCherry-MUT within single living cells. As shown in Figure 4A, in the EGFP-Ub-p53-mCherry-ΔGG, the $G(0)$ of the CCF curve (black curve) was close to the $G(0)$ of the ACF curve (blue curve). Then, the determined DU % of p53 protein in the locations (arrow) is 3.5%. Also, the average DU % results (Figure 4C) showed that their DU % [(8.0 ± 6.0)%] is far less than that in the EGFP-Ub-p53-mCherry [(83.0 ± 8.5)%]. It indicated that almost no Ub can be removed from p53 by endogenous DUBs in living cells due the lack of Ub C-terminal Gly75-Gly76 motif. This result is consistent with the reported study.[51]

Meanwhile, when the Ile44 hydrophobic patch of Ub was mutated (EGFP-Ub-p53-mCherry-MUT), the DU% in a single cell is 19.3% (Figure 4B), which is significantly higher than that of ΔGG. As shown in Figure 4C, the average DU % was (20.0 ± 15.7)% and was larger than that of EGFP-Ub-p53-mCherry-ΔGG [(8.0 ± 6.0)%]. This data indicated that although Ile44 hydrophobic patch is also significant in the deubiquitination process, the part of Ub can still be removed from p53 protein. It was reported that, in this cleavage, some DUBs can directly execute the deubiquitination process without interacting with the Ile44 hydrophobic patch of p53 protein.[52]

The above results further confirmed that the C-terminal Gly−Gly motif and Ile44 hydrophobic patch of Ub both play a significant role in maintaining the deubiquitination activity of Ub. Our results further illustrated that FCCS is very suitable to study deubiquitination in living cells.

CONCLUSIONS

In this work, we proposed an in situ strategy for monitoring the deubiquitination process of proteins in a single living cell using p53 protein as a model by combining FCCS with a fluorescent protein labeling technique. In this study, based on the amplitudes of FCS and FCCS curves from living cells, we can calculate the DU % for evaluating the level of p53 protein deubiquitination. We studied the effects of Ub structures on deubiquitination, and our results further confirmed that the C-terminal Gly−Gly motif and Ile44 hydrophobic patch of Ub both play a significant role in maintaining the deubiquitination activity of Ub. Our preliminary results illustrated that FCCS is more suitable to study deubiquitination in single living cells compared to the fluorescence colocalization imaging technique. FCCS may become an important tool to study the candidate drugs for adjusting the deubiquitination process.

ASSOCIATED CONTENT

Supporting Information

The Supporting Information is available free of charge on the ACS Publications Web site. The Supporting Information is available free of charge at https://pubs.acs.org/doi/10.1021/acsomega.3c06078.

Western blot analysis, FCS/FCCS system, and study of monoclonal cell line of EGFP-Ub-p53-mCherry (PDF)

AUTHOR INFORMATION

Corresponding Authors

Chaoqing Dong − *School of Chemistry and Chemical Engineering, State Key Laboratory of Metal Matrix Composites, Shanghai Jiao Tong University, Shanghai 200240, People's Republic of China;* orcid.org/0000-0002-6457-1975; Email: cqdong@sjtu.edu.cn

Jicun Ren − *School of Chemistry and Chemical Engineering, State Key Laboratory of Metal Matrix Composites, Shanghai Jiao Tong University, Shanghai 200240, People's Republic of China;* orcid.org/0000-0002-8157-5548; Email: jicunren@sjtu.edu.cn

Author

Yaoqi Liu − *School of Chemistry and Chemical Engineering, State Key Laboratory of Metal Matrix Composites, Shanghai Jiao Tong University, Shanghai 200240, People's Republic of China*

Complete contact information is available at: https://pubs.acs.org/10.1021/acsomega.3c06078

Author Contributions

All authors have given approval to the final version of the manuscript.

Notes

The authors declare no competing financial interest.

ACKNOWLEDGMENTS

We gratefully acknowledge funding from the National Natural Science Foundation of China (grant nos. 22274098, 22027803, 21834005, 21874090), the Shanghai Natural Science Foundation (grant no. 22ZR1429300), Key Project of Basic Research of Shanghai (18JC1413400), and the Development Fund for Shanghai Talents (2020031).

REFERENCES

(1) Komander, D.; Rape, M. The ubiquitin code. *Annu. Rev. Biochem.* **2012**, *81*, 203−229.

(2) Grabbe, C.; Dikic, I. Functional roles of ubiquitin-like domain (ULD) and ubiquitin-binding domain (UBD) containing proteins. *Chem. Rev.* **2009**, *109*, 1481−1494.

(3) Komander, D.; Clague, M. J.; Urbé, S. Breaking the chains: structure and function of the deubiquitinases. *Nat. Rev. Mol. Cell Biol.* **2009**, *10*, 550−563.

(4) Elsasser, S.; Finley, D. Delivery of ubiquitinated substrates to protein-unfolding machines. *Nat. Cell Biol.* **2005**, *7*, 742−749.

(5) Staub, O.; Rotin, D. Role of ubiquitylation in cellular membrane transport. *Physiol. Rev.* **2006**, *86*, 669−707.
(6) Huang, T. T.; D'Andrea, A. D. Regulation of DNA repair by ubiquitylation. *Nat. Rev. Mol. Cell Biol.* **2006**, *7*, 323−334.
(7) Bergink, S.; Jentsch, S. Principles of ubiquitin and SUMO modifications in DNA repair. *Nature* **2009**, *458*, 461−467.
(8) Raiborg, C.; Bache, K. G.; Gillooly, D. J.; Madshus, I. H.; Stang, E.; Stenmark, H. Hrs sorts ubiquitinated proteins into clathrin-coated microdomains of early endosomes. *Nat. Cell Biol.* **2002**, *4*, 394−398.
(9) Haglund, K.; Dikic, I. Ubiquitylation and cell signaling. *EMBO J.* **2005**, *24*, 3353−3359.
(10) Levine, A. J.; Oren, M. The first 30 years of p53: growing ever more complex. *Nat. Rev. Cancer* **2009**, *9*, 749−758.
(11) Vousden, K. H.; Prives, C. Blinded by the Light: The Growing Complexity of p53. *Cell* **2009**, *137*, 413−431.
(12) Ladds, M.; Laín, S. Small molecule activators of the p53 response. *J. Mol. Cell Biol.* **2019**, *11*, 245−254.
(13) Kruse, J. P.; Gu, W. Modes of p53 regulation. *Cell* **2009**, *137*, 609−622.
(14) Gu, B.; Zhu, W. G. Surf the post-translational modification network of p53 regulation. *Int. J. Biol. Sci.* **2012**, *8*, 672−684.
(15) Liu, J.; Guan, D.; Dong, M.; Yang, J.; Wei, H.; Liang, Q.; Song, L.; Xu, L.; Bai, J.; Liu, C.; Mao, J.; Zhang, Q.; Zhou, J.; Wu, X.; Wang, M.; Cong, Y. S. UFMylation maintains tumour suppressor p53 stability by antagonizing its ubiquitination. *Nat. Cell Biol.* **2020**, *22*, 1056−1063.
(16) Chao, C. C. Mechanisms of p53 degradation. *Clin. Chim. Acta* **2015**, *438*, 139−147.
(17) Du, Z.; Yu, J.; Li, F.; Deng, L.; Wu, F.; Huang, X.; Bergstrand, J.; Widengren, J.; Dong, C.; Ren, J. In Situ Monitoring of p53 Protein and MDM2 Protein Interaction in Single Living Cells Using Single-Molecule Fluorescence Spectroscopy. *Anal. Chem.* **2018**, *90*, 6144−6151.
(18) Kwon, S. K.; Saindane, M.; Baek, K. H. p53 stability is regulated by diverse deubiquitinating enzymes. *Biochim. Biophys. Acta, Rev. Cancer* **2017**, *1868*, 404−411.
(19) Li, M.; Chen, D.; Shiloh, A.; Luo, J.; Nikolaev, A. Y.; Qin, J.; Gu, W. Deubiquitination of p53 by HAUSP is an important pathway for p53 stabilization. *Nature* **2002**, *416*, 648−653.
(20) Stevenson, L. F.; Sparks, A.; Allende-Vega, N.; Xirodimas, D. P.; Lane, D. P.; Saville, M. K. The deubiquitinating enzyme USP2a regulates the p53 pathway by targeting Mdm2. *EMBO J.* **2007**, *26*, 976−986.
(21) Yuan, J.; Luo, K.; Zhang, L.; Cheville, J. C.; Lou, Z. USP10 regulates p53 localization and stability by deubiquitinating p53. *Cell* **2010**, *140*, 384−396.
(22) Gopinath, P.; Ohayon, S.; Nawatha, M.; Brik, A. Chemical and semisynthetic approaches to study and target deubiquitinases. *Chem. Soc. Rev.* **2016**, *45*, 4171−4198.
(23) Whedon, S. D.; Markandeya, N.; Rana, A.; Senger, N. A.; Weller, C. E.; Tureček, F.; Strieter, E. R.; Chatterjee, C. Selenocysteine as a Latent Bioorthogonal Electrophilic Probe for Deubiquitylating Enzymes. *J. Am. Chem. Soc.* **2016**, *138*, 13774−13777.
(24) Vassilev, L. T.; Vu, B. T.; Graves, B.; Carvajal, D.; Podlaski, F.; Filipovic, Z.; Kong, N.; Kammlott, U.; Lukacs, C.; Klein, C.; Fotouhi, N.; Liu, E. A. In vivo activation of the p53 pathway by small-molecule antagonists of MDM2. *Science* **2004**, *303*, 844−848.
(25) Das, A.; Yadav, A.; Gupta, M.; R, P.; Terse, V. L.; Vishvakarma, V.; Singh, S.; Nandi, T.; Banerjee, A.; Mandal, K.; Gosavi, S.; Das, R.; Ainavarapu, S. R. K.; Maiti, S. Rational Design of Protein-Specific Folding Modifiers. *J. Am. Chem. Soc.* **2021**, *143*, 18766−18776.
(26) Li, H.; Liu, Y.; Zhang, J.; Cai, M.; Cao, Z.; Gao, J.; Xu, H.; Shao, L.; Sun, J.; Shi, Y.; Wang, H. Quantification of mechanical stimuli inducing nucleoplasmic translocation of YAP and its distribution mechanism using an AFM-dSTORM coupled technique. *Nanoscale* **2022**, *14*, 15516−15524.
(27) Dziuba, D.; Didier, P.; Ciaco, S.; Barth, A.; Seidel, C. A. M.; Mély, Y. Fundamental photophysics of isomorphic and expanded fluorescent nucleoside analogues. *Chem. Soc. Rev.* **2021**, *50*, 7062−7107.
(28) Han, M.-J.; He, Q.-t.; Yang, M.; Chen, C.; Yao, Y.; Liu, X.; Wang, Y.; Zhu, Z.-l.; Zhu, K.-k.; Qu, C.; Yang, F.; Hu, C.; Guo, X.; Zhang, D.; Chen, C.; Sun, J.-p.; Wang, J. Single-molecule FRET and conformational analysis of beta-arrestin-1 through genetic code expansion and a Se-click reaction. *Chem. Sci.* **2021**, *12*, 9114−9123.
(29) Wang, Z.-Y.; Li, P.; Hu, J.; Xu, Q.; Zhang, C.-y. Construction of a Single-Molecule Biosensor for Antibody-Free Detection of Locus-Specific N6-Methyladenosine in Cancer Cells and Tissues. *Anal. Chem.* **2023**, *95*, 5454−5462.
(30) Krieger, J. W.; Singh, A. P.; Bag, N.; Garbe, C. S.; Saunders, T. E.; Langowski, J.; Wohland, T. Imaging fluorescence (cross-) correlation spectroscopy in live cells and organisms. *Nat. Protoc.* **2015**, *10*, 1948−1974.
(31) Li, F.; Du, Z.; Huang, X.; Dong, C.; Ren, J. Analyses of p73 Protein Oligomerization and p73-MDM2 Interaction in Single Living Cells Using In Situ Single Molecule Spectroscopy. *Anal. Chem.* **2021**, *93*, 886−894.
(32) Peng, S.; Wang, X.; Zhang, L.; He, S.; Zhao, X. S.; Huang, X.; Chen, C. Target search and recognition mechanisms of glycosylase AlkD revealed by scanning FRET-FCS and Markov state models. *Proc. Natl. Acad. Sci. U.S.A.* **2020**, *117*, 21889−21895.
(33) Sandberg, E.; Piguet, J.; Kostiv, U.; Baryshnikov, G.; Liu, H.; Widengren, J. Photoisomerization of Heptamethine Cyanine Dyes Results in Red-Emissive Species: Implications for Near-IR, Single-Molecule, and Super-Resolution Fluorescence Spectroscopy and Imaging. *J. Phys. Chem. B* **2023**, *127*, 3208−3222.
(34) Sankaran, J.; Balasubramanian, H.; Tang, W. H.; Ng, X. W.; Röllin, A.; Wohland, T. Simultaneous spatiotemporal super-resolution and multi-parametric fluorescence microscopy. *Nat. Commun.* **2021**, *12*, 1748.
(35) Du, Z.; Dong, C.; Ren, J. A study of the dynamics of PTEN proteins in living cells using in vivo fluorescence correlation spectroscopy. *Methods Appl. Fluoresc.* **2017**, *5*, 024008.
(36) Dunn, K. W.; Kamocka, M. M.; McDonald, J. H. A practical guide to evaluating colocalization in biological microscopy. *Am. J. Physiol. Cell Physiol.* **2011**, *300*, C723−C742.
(37) Schwille, P.; Haupts, U.; Maiti, S.; Webb, W. W. Molecular dynamics in living cells observed by fluorescence correlation spectroscopy with one- and two-photon excitation. *Biophys. J.* **1999**, *77*, 2251−2265.
(38) Haupts, U.; Maiti, S.; Schwille, P.; Webb, W. W. Dynamics of fluorescence fluctuations in green fluorescent protein observed by fluorescence correlation spectroscopy. *Proc. Natl. Acad. Sci. U.S.A.* **1998**, *95*, 13573−13578.
(39) Weiss, M.; Elsner, M.; Kartberg, F.; Nilsson, T. Anomalous subdiffusion is a measure for cytoplasmic crowding in living cells. *Biophys. J.* **2004**, *87*, 3518−3524.
(40) Banks, D. S.; Fradin, C. Anomalous diffusion of proteins due to molecular crowding. *Biophys. J.* **2005**, *89*, 2960−2971.
(41) Pack, C. G.; Nishimura, G.; Tamura, M.; Aoki, K.; Taguchi, H.; Yoshida, M.; Kinjo, M. Analysis of interaction between chaperonin GroEL and its substrate using fluorescence correlation spectroscopy. *Cytometry* **1999**, *36*, 247−253.
(42) Krichevsky, O.; Bonnet, G. Fluorescence correlation spectroscopy: the technique and its applications. *Rep. Prog. Phys.* **2002**, *65*, 251−297.
(43) Bacia, K.; Schwille, P. Practical guidelines for dual-color fluorescence cross-correlation spectroscopy. *Nat. Protoc.* **2007**, *2*, 2842−2856.
(44) Levine, A. J. p53, the cellular gatekeeper for growth and division. *Cell* **1997**, *88*, 323−331.
(45) Swatek, K. N.; Aumayr, M.; Pruneda, J. N.; Visser, L. J.; Berryman, S.; Kueck, A. F.; Geurink, P. P.; Ovaa, H.; van Kuppeveld, F. J. M.; Tuthill, T. J.; Skern, T.; Komander, D. Irreversible inactivation of ISG15 by a viral leader protease enables alternative infection detection strategies. *Proc. Natl. Acad. Sci. U.S.A.* **2018**, *115*, 2371−2376.

https://doi.org/10.1021/acsomega.3c06078
ACS Omega 2023, 8, 36588−36596

(46) Cappadocia, L.; Lima, C. D. Ubiquitin-like Protein Conjugation: Structures, Chemistry, and Mechanism. *Chem. Rev.* **2018**, *118*, 889−918.
(47) Swatek, K. N.; Usher, J. L.; Kueck, A. F.; Gladkova, C.; Mevissen, T. E. T.; Pruneda, J. N.; Skern, T.; Komander, D. Insights into ubiquitin chain architecture using Ub-clipping. *Nature* **2019**, *572*, 533−537.
(48) Dikic, I.; Wakatsuki, S.; Walters, K. J. Ubiquitin-binding domains - from structures to functions. *Nat. Rev. Mol. Cell Biol.* **2009**, *10*, 659−671.
(49) Hicke, L.; Schubert, H. L.; Hill, C. P. Ubiquitin-binding domains. *Nat. Rev. Mol. Cell Biol.* **2005**, *6*, 610−621.
(50) Cappadocia, L.; Lima, C. D. Ubiquitin-like Protein Conjugation: Structures, Chemistry, and Mechanism. *Chem. Rev.* **2018**, *118*, 889−918.
(51) Komander, D.; Clague, M. J.; Urbé, S. Breaking the chains: structure and function of the deubiquitinases. *Nat. Rev. Mol. Cell Biol.* **2009**, *10*, 550−563.
(52) Reyes-Turcu, F. E.; Horton, J. R.; Mullally, J. E.; Heroux, A.; Cheng, X.; Wilkinson, K. D. The Ubiquitin Binding Domain ZnF UBP Recognizes the C-Terminal Diglycine Motif of Unanchored Ubiquitin. *Cell* **2006**, *124*, 1197−1208.

https://doi.org/10.1021/acsomega.3c06078
ACS Omega 2023, 8, 36588−36596